İSTANBUL TECHNICAL UNIVERSITY ★ INSTITUTE OF SCIENCE AND TECHNOLOGY

ELECTROMAGNETIC IMAGING OF CONDUCTING OBJECTS BURIED UNDER A HALF SPACE BY AN INTEGRAL EQUATION APPROACH

M.Sc. Thesis by

Umut Aziz ALBAYRAK, B.Sc.

Department : Electronics and Communication Engineering

Programme : Telecommunication Engineering

OCTOBER 2008

İSTANBUL TECHNICAL UNIVERSITY ★ INSTITUTE OF SCIENCE AND TECHNOLOGY

ELECTROMAGNETIC IMAGING OF CONDUCTING OBJECTS BURIED UNDER A HALF SPACE BY AN INTEGRAL EQUATION APPROACH

M.Sc. Thesis by

Umut Aziz ALBAYRAK, B.Sc.

(504041327)

Date of submission : 15 September 2008

Date of examin : 08 October 2008

Supervisor (Chairman): Assoc. Prof. Dr. Ali YAPAR

Members of the Examining Committee Prof. Dr. İbrahim AKDUMAN (İ.T.Ü.)

Assist. Prof. Dr. Lale T. ERGENE (İ.T.Ü.)

OCTOBER 2008

İSTANBUL TECHNICAL UNIVERSITY ★ INSTITUTE OF SCIENCE AND TECHNOLOGY

YERALTINA GÖMÜLÜ CİSMİN ŞEKLİNİN İNTEGRAL METOT YARDIMIYLA BELİRLENMESİ

YÜKSEK LİSANS TEZİ

Müh. Umut Aziz ALBAYRAK

(504041327)

Tezin Enstitüye Verildiği Tarih : 15 Eylül 2008

Tezin Savunulduğu Tarih : 08 Ekim 2008

Tez Danışmanı: Doç. Dr. Ali YAPAR

Diğer Jüri Üyeleri Prof. Dr. İbrahim AKDUMAN (İ.T.Ü.)

Yrd. Doç. Dr. Lale T. ERGENE (İ.T.Ü.)

EKİM 2008

ACKNOWLEDGEMENT

I would like to express my immense gratitude to Assoc. Prof. Dr. Ali YAPAR, who gave me the opportunity to do research under his supervision, for his precious guidance and support during this study.

I also owe my thanks to Electromagnetic Research Group, İ.T.Ü. for their support in every step of this research, and of course to my mother and my father for their endless love and their faith in me.

October, 2008 Umut Aziz ALBAYRAK

TABLE OF CONTENT

LIST OF FIGURES

LIST OF SYMBOLS

ε_0	: Dielectric permittivity of the free space
μ_0	: Magnetic permeability of the free space
$\varepsilon_1, \varepsilon_2$	: Relative dielectric permittivities of the first, second media
ε_D	: Relative dielectric permittivity of the buried object
σ_1, σ_2	: Conductivities of first, second media
σ_D	: Conductivity of the buried object
k_1, k_2	: Wavenumber of the first, second media
ω	: Angular frequency
u^0	: Total field in whole space in the absence of the buried objects
u	: Total field
u^s	: Scattered field
χ	: Object function
G	: Green's function of the two part space
$\hat{G}$	: Fourier transform of G
r	: generic observation point
r'	: generic source point
δ	: Dirac delta distribution
σ_n	: singular values
$\hat{u}^s(v, x_2)$	: Fourier transform of $u^s(x_1,x_2)$
A	: radiation condition

ELECTROMAGNETIC IMAGING OF CONDUCTING OBJECTS BURIED UNDER A HALF SPACE BY AN INTEGRAL EQUATION APPROACH

SUMMARY

In this thesis an iterative method is applied to determine the location and shape of a perfectly conducting object buried under a half space. First of all, we express the scattered field in the upper half space. Then we express the scattered field at the half space interface by using continuous method. After expressing the scattered field at the half space interface, we investigate an iterative method for electromagnetic imaging of conducting objects buried under a half space. The method starts with an initial guess of the shape of the boundary curve of the obstacle. Then, the normal derivative of the space dependent part of the total acoustic field is found on this curve from a linear integral equation of the first kind with a singular kernel representing the incident field. Once this derivative is known, the shape of the boundary curve is updated from a nonlinear integral equation which represents the far-field pattern. The normal derivative of the space-dependent part of the total acoustic field is found on this updated curve by again solving the linear integral equation which represents the incident field. The iterative procedure is continued until a predetermined convergency condition is fulfilled. And continuing in this manner, a sequence of approximations of the boundary curve of the obstacle is found. Also in this thesis, we will see the effects of some parameters while we are expressing the scattered data at the half space interface or finding the shape of the object.

The comparison of the results with the examples given in the literature was in a good agreement.

YERALTINA GÖMÜLÜ İLETKEN CİSİMLERİN ŞEKLİNİN İNTEGRAL METOT YARDIMIYLA BELİRLENMESİ

ÖZET

Bu tezde, yarım düzlem altına gömülü çok iyi iletken bir cismin şeklini ve yerini belirlemek için tekrarlayıcı(yineleyici) bir method kullanacağız. İlk başta yansıyan alanın üst yarı düzlemdeki ifadesini bulacağız. Daha sonra yansıyan alanın yarı düzlem arayüzeyindeki ifadesini analitik süreklilik metodunu kullanarak bulacağız. Yansıyan alanı yarı düzlem arayüzeyinde ifade ettikten sonra yeraltına gömülü cisimlerin şeklinin belirlenmesi için tekrarlayıcı(yineleyici) bir method kullanacağız. Methodumuz, ilk başta yeraltına gömülü cisim için kendimize göre bir kapalı eğri belirleyerek başlıyor. Daha sonra belirlediğimiz kapalı eğri üzerindeki alan lineer integral denklemler(kernel) vasıtasıyla bulunur.Bu alanı belirledikten sonrada lineer olmayan integral denklemler yardımı ile de ilk başta kendimize göre atadığımız kapalı eğriyi güncelleyeceğiz. Daha sonra tekrar güncellediğimiz eğrinin üzerindeki alanı lineer denklemler yardımı ile buluruz. Ve bu şekilde ilerleyerek(tekrarlayarak) ilk başta kendimize göre atadığımız şekli güncelleriz. İteratif(tekrarlayıcı) prosedür elde ettiğimiz şekiller birbirine yakınsayana kadar devam eder. Belli bir adımdan sonra elde ettiğimiz sonuçlar birbirlerine yaklaşık olarak eşit olduklarında yinelemeyi bitiririz. Ve gömülü cismin şeklini belirlemiş oluruz. Ayrıca bu tezde yansıyan alanın yarı düzlem arayüzeyindeki ifadesini bulurken veya cismin şeklini belirlemeye çalışırken bazı parametrelerin elde ettiğimiz sonuçlara etkilerinide göreceğiz.

Sonuçları literatürdeki çalışmalarla karşılaştırdığımızda, önerilen yöntemlerle elde edilen sonuçlar mühendislik açısından yeter yakınsaklığı sağladığı gözlenmiştir.

1. INTRODUCTION

Electromagnetic scattering from objects has been an area of in depth research for many years. A variety of powerful solution methodologies have been developed and utilized for the clever solution of increasingly complex problems.

The electromagnetic direct scattering problem is the problem of determining the scattered field when the geometrical and physical properties of the scatterer are known. Thus, there many books and papers have been published about scattering of electromagnetic waves. On the other hand, inverse scattering is the problem of inferring information on the source of the known scattering field data. Practically, this data is obtained via measurements in a particular domain. However, in order to test the reconstruction algorithms the data can be obtained synthetically by solving the direct problem, which is case in this proposed thesis.

Reconstruction of the shape of a conducting object by using electromagnetic or acoustic waves is one of the fundamental problems of inverse scattering theory not only for its mathematical and physical importance but also for the wide range of applications in the areas of microwave remote sensing, optical system measurements, underwater acoustics and non-destructive testing of materials etc. Additionally, various medical imaging applications are concerned with reconstructing the inhomogeneities by solving the arisen inverse scattering problems.

Within this framework another interesting problem would be the imaging of conducting objects buried under a half space by an integral equation approach. In this work an iterative method is applied to determine the location and shape of a perfectly conducting object buried under a half space which is not widely investigated in the open literature as far as we know.

The organization of the thesis is as follows: In section 2, a general formulation of the inverse scattering problem is formulated. In section 3, we express the scattered field at the half-space interface. In section 4, we investigate an iterative method for electromagnetic imaging of conducting objects buried under a half space. The

method starts with an initial guess of the shape of the boundary curve of the obstacle. Then, the normal derivative of the space-dependent part of the total acoustic field is found on this curve from a linear integral equation of the first kind with a singular kernel representing the incident field. Once this derivative is known, the shape of the boundary curve is updated from a nonlinear integral equation which represents the far-field pattern. The normal derivative of the space-dependent part of the total acoustic field is found on this updated curve by again solving the linear integral equation which represents the incident field. Numerical results are given in section 5, and a conclusion is presented in section 6.

2. GENERAL FORMULATION OF THE PROBLEM

Consider the geometry given in Figure 1. Here D is a perfectly conducting object buried in the lower half space. The object is illuminated from the upper half space and the scattered field is measured on a limited line parallel to the interface. The inverse problem considered here is to obtain the geometry of the buried conducting object D, i.e; ∂D, by the use of measurements performed in a planar domain inside the upper half space.

To formulate the problem in an appropriate way, first decompose the total field as, $u(x) = u^o(x) + u^s(x), \quad (x = (x_1, x_2) \in R^2)$ where u^o corresponds to the total field in

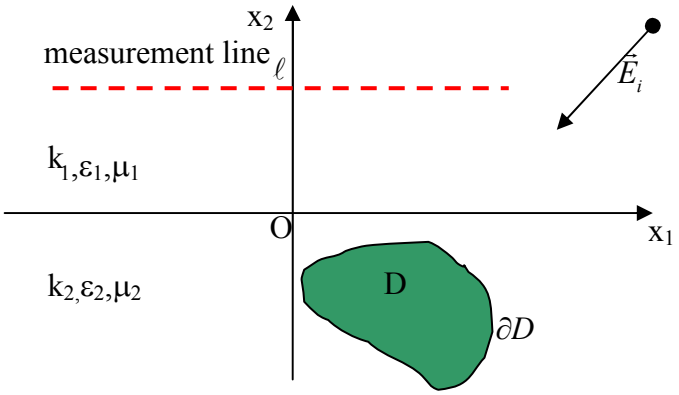

Figure 2.1 - Geometry of the Problem

the absence of the buried object, while u^s denotes the scattered field due to the conducting buried object. Then by the use of Fourier Transform one can represent the scattered field in the upper half-space as [1]

$$u^s(x_1, x_2) = \frac{1}{2\pi} \int_\Gamma A(\upsilon) e^{-\gamma(\upsilon)x_2} e^{i\upsilon x_1} d\upsilon \qquad (2.1)$$

In which $A(\upsilon)$ is the unknown spectral coefficient while $\gamma(\upsilon) = \sqrt{\upsilon^2 - k_1^2}$ is the properly defined square root function in the complex-υ plane, where k_1 is the wave

number of the upper half-space. Now assume that the scattered field is measured on a line $x_2 = \ell > 0$, parallel to the half space interface. Then putting $x_2 = \ell$ in (2.1) one can calculate the unknown spectral coefficient by inverting the integral equation (2.1). Once having obtained this coefficient it is easy to express the scattered field at the half-space interface by just putting $x_2 = 0$ in (2.1).

The second step of our algorithm is to represent the scattered field in the lower half-space as a single layer potential which leads to the following integral equation in terms of the field values $u^s(x_1, 0)$

$$u^s(x_1, 0) = \int_{\partial D} G(x, y)\Phi(y)\, ds(y) \tag{2.2}$$

where $G(x,y) = \frac{i}{4} H_0^{(1)}(k_2 |x - y|)$ is the Green's function with k_2 being the wave number of the lower half-space and $\Phi(y)$ is the unknown single layer density function. In (2) both the shape of the scatterer and the density function are unknowns. The boundary condition on the surface of the body can be written as

$$u^s(x) = -u^o(x), \quad x \in \partial D \tag{2.3}$$

Equations (2.2) and (2.3) constitute a system of non-linear equations in terms of two unknowns $\Phi(y)$ and ∂D. Now following a similar approach presented in [1], this system can be solved iteratively. To this aim we first solve (2.3) by Nyström method for a given initial estimate of the shape $\partial D^{(0)}$ to obtain an approximate density function $\Phi^{(0)}(y)$. Then the parametric form of the equation (2.2) is linearized in the sense of Newton method which requires the Frechét derivative of the operator with respect to the shape of the object. The solution of the linearized equation gives us the updated shape, say, $\partial D^{(1)}$. The iterative procedure explained above is continued until a predetermined convergency condition is fulfilled. It is worth to note that in the application of the method some regularization techniques have been applied since in both steps the problem encountered are ill-posed.

3. DIRECT SCATTERİNG PROBLEM

3.1 Direct Scattering Problem

Consider the two-dimensional scattering problem illustrated in Figure 2.1. In this configuration, the whole space is separated into two half-spaces by the interface Γo, which is defined by the relation $x_2 = f(x_1)$ where $f(x_1)$ is a single-valued function. Γo is assumed to be locally smoth, i.e., $f(x_1)$ differs from the planar surface over a finite interval whose length is L.The half-spaces above and below Γo are assumed to be filled with simple nonmagnetic materials having dielectric permittivities and conductivities ε_1, σ_1 and ε_2, σ_2 respectively. The scattering problem considered here is to determine the effect of Γo on the propagation of electromagnetic waves excited in the upper half-space $x_2 > f(x_1)$, more precisely, to obtain the scattered field from the surface Γo. To this aim, the half-space $x_2 < f(x_1)$ is illuminated by a time-harmonic plane wave whose electric-field vector is always parallel to the $0x_3$ axis, namely,

$$E_i = (0, 0, u_i(x_1, x_2)) \tag{3.1}$$

$$u_i(x_1, x_2) = e^{-ik_1 (x_1 \cos\phi_0 + x_2 \sin\phi_0)} \tag{3.2}$$

where $\phi 0 \in (0, \pi)$ is the angle of incidence while k_1 stands for the wave number of the upper half-space, which is defined by the square root of $k_{12} = \omega_2 \varepsilon_1 \mu_0 + i\omega\sigma_1\mu_0$. Since the problem is homogeneous in the $0x_3$ direction, the total electric-field vector will also be parallel to the *Ox3-axis,* namely, E = (0, 0, u(x)), where x = (x1,x2) denotes the position vector in $\Re 2$. Thus, the problem is reduced to a scalar one in terms of the total field function u(x).

To solve the scattering problem stated above, we first assume that the whole space is separated into two parts by the plane $x_2 = 0$. In such a case, the half-spaces $x_2 > 0$ and $x_2 < 0$ contain 2 finite domains bounded by the Γo and $x_2 = 0$ plane. Let us denote the ones in the region $x_2 > 0$ by D_1 and the rest in the region $x_2 < 0$ by D_1 . Note that

the dielectric permittivities and conductivities of the regions D_1 and D_2 are ε_1, σ_1 and ε_2, σ_2 respectively.

To formulate the problem more easily, consider now the total field $u_0(x)$ that would be created by the incident field (3.1) in the case of two-half spaces medium separated by the plane $x_i = 0$ (See Fig. 3.1.) In this case $u_0(x)$ can be obtained in a very straightforward way.

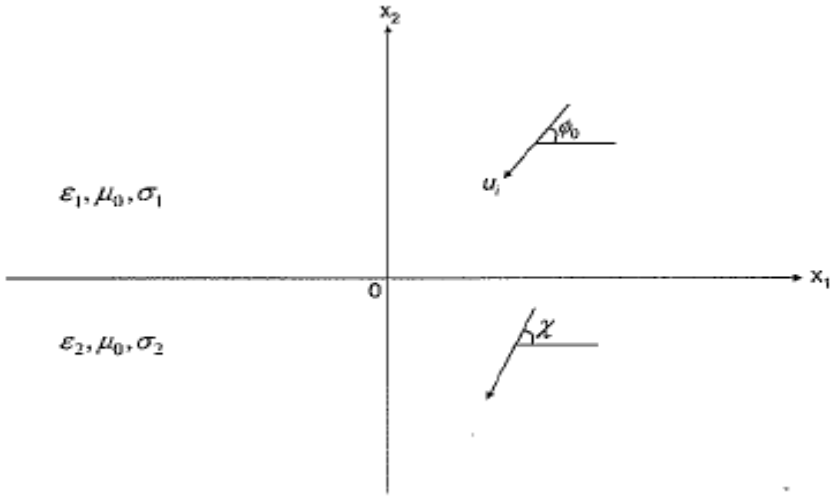

Figure 3.1 – Geometry for the field u_0

$U_s(x)$, consists in the difference

$$u_s(x) = u(x) - u_0(x) \tag{3.3}$$

can be expresssed as a single layer potential integral as follows

$$u_s(x) = \int_0^{\infty} G(x;y)\,\psi(y)ds(y) \tag{3.4}$$

where G(x;y) denotes the Green's function of the two-part space with a planar interface at $x_2 = 0$, and $\psi(y)$ is the unknown density function. The solution of the direct scattering can be reduced to the solution of the unknown density function. The valid boundary condition on the surface of the buried PEC object is $u_s(x) = -u_0(x)$.

From (3.3) and (3.4) we can express

$$\int_{\partial D} G(x;y)\psi(y)ds(y) = -u_0(x)$$

3.2 Green's Function of the two-part space

By definition, the Green's function G(x;y) satisfies the equation

$$\Delta G(x;y) + k^2 (x_2)\, G(x;y) = -\delta(x-y) \tag{3.5}$$

in the sense of distributions under the radiation condition. In this equation, y € R^2 is an arbitrary point and δ is the Dirac's delta distribution.

To find a suitable expression of G, consider first its Fourier transform with respect to x_1, namely,

$$G^{\wedge}(v, x_2; y) = \int_{-\infty}^{\infty} G(X;Y) e^{-ivx_1} dx_1 \tag{3.6}$$

Then the transformations of (3.5) and the boundary conditions at $x_2 = 0$ yield the following problem for G^:

$$\frac{d^2 G^{\wedge}}{dx_2^2} - (v^2 - k_j^2) G^{\wedge} = -e^{ivy_1} \delta(x_2 - y_2), \quad j = 1,2, \quad v \in C_R \tag{3.7}$$

$$G^{\wedge} \text{ and } \frac{\partial G^{\wedge}}{\partial x_2} \text{ are continuous on } x_2 = 0 \tag{3.8}$$

$$|G| \rightarrow 0 \quad \text{as } |x| \rightarrow \infty \tag{3.9}$$

Here, C_R stands for a horizontal straight line in the regularity strip of G^ in the complex v-plane(see figure3.2). After some straightforward calculations and through the well-known inverse transform integral

$$G(x;y) = \frac{1}{2\pi} \int_{C_R} G^{\wedge}(v, x_2; y)\, e^{-ivx_1} dv \tag{3.10}$$

We can get an explicit expression of G(x; y) as follows:

$$G(x;y) = \begin{cases} \frac{i}{4} H_0^{(1)}(k_1 \mid x-y \mid) + G_R^{(1)}(x;y); & x_2 > 0,\ y_2 > 0 \\ G_T^{(1)}(x;y); & x_2 < 0,\ y_2 > 0 \\ G_T^{(2)}(x;y); & x_2 > 0,\ y_2 < 0 \\ \frac{i}{4} H_0^{(1)}(k_2 \mid x-y \mid) + G_R^{(2)}(x;y); & x_2 < 0,\ y_2 < 0 \end{cases} \tag{3.11}$$

Where

$$G_R^{(1)}(x;y) = \frac{1}{2\pi} \int_{C_R} \frac{1}{2\gamma_1} \frac{\gamma_1 - \gamma_2}{\gamma_1 + \gamma_2} e^{-\gamma_1(x_2+y_2)} e^{iv(x_1-y_1)} dv \tag{3.12}$$

$$G_T^{(1)}(x;y) = \frac{1}{2\pi} \int_{C_R} \frac{1}{2\gamma_1} \frac{2\gamma_1}{\gamma_1 + \gamma_2} e^{-\gamma_1 y_2 + \gamma_2 x_2} e^{iv(x_1-y_1)} dv \tag{3.13}$$

$$G_T^{(2)}(x;y) = \frac{1}{2\pi} \int_{C_R} \frac{1}{2\gamma_2} \frac{2\gamma_2}{\gamma_1 + \gamma_2} e^{\gamma_2 y_2 + \gamma_1 x_2} e^{iv(x_1-y_1)} dv \tag{3.14}$$

$$G_R^{(2)}(x;y) = \frac{1}{2\pi} \int_{C_R} \frac{1}{2\gamma_2} \frac{\gamma_2 - \gamma_1}{\gamma_1 + \gamma_2} e^{-\gamma_2(x_2+y_2)} e^{iv(x_1-y_1)} dv \tag{3.15}$$

While $H_0^{(1)}$ zero-order Hankel function of the first kind. In (3.12)-(3.15) the functions γ_1 and γ_2 stand for the square roots

$$\gamma_1(v) = \sqrt{v^2 - k_1^2}, \quad \gamma_2(v) = \sqrt{v^2 - k_2^2} \tag{3.16}$$

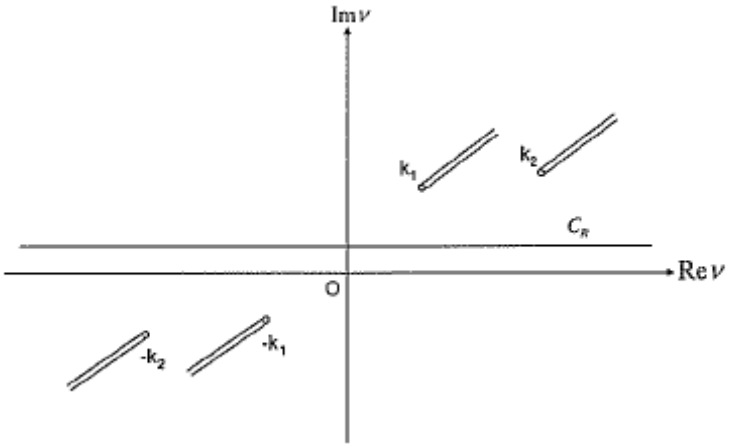

Figure 3.2 – Complex v plane

Which are defined in the complex v-plane cut as shown in Figure3 with the conditions

$$\gamma_j(0) = -ik_j, \quad j = 1,2 \tag{3.17}$$

From the (3.12), (3.15) and (3.11) we can easily see that G is symmetrical, and has the property

$$G(x,y) = G\hat{}(|x_1-y_1|, x_2,y_2), \qquad x,y \in \Re^2 \tag{3.18}$$

4. INVERSE SCATTERİNG AND ITERATIVE METHOD

4.1 Formulation Of the Inverse Scattering Problem

In figure (2.1), assume that scattered field is measured in the line $x_2 = l$. The inversede problem defined here is to obtain the shape of the scatterer ∂D from the knowledge of this scattered data.Scattered field on $x_2 = l$ is,

$$u^s(x_1, l) = \int_{\partial D} G(x, y)\psi(y)ds(y) \tag{4.1}$$

But as we can see form the section 3, it is very complex and hard to solve it. Because of this we can carry the data from $x_2 = l$ to $x_2 = 0$ and we can write (4.1) as

$$u^s(x_1, 0) = \int_{\partial D} H_0^{(1)}(k_2 |x - y|\psi_y ds(y) \tag{4.2}$$

And let $\hat{u}^s(v, x_2)$ denote the Fourier transform of $\hat{u}(v, x_2)$ with the respect to x_2, namely,

$$\hat{u}^s(v, x_2) = \int_{-\infty}^{\infty} u^s(x_1, x_2)e^{-ivx_1}dx_1, \qquad v \in L,\ x_2 > 0 \tag{4.3}$$

which yields,

$$u^s(x_1, x_2) = \frac{1}{2\pi} \int_L \hat{u}^s(v, x_2)e^{ivx_1}dv \tag{4.4}$$

Here L stands for a horizontal straight line in the regulatory strip of $\hat{u}^s$ in the complex v plane. The asymptotic behavior of $u^s(x_1, x_2)$ as $x_1 \to \pm\infty$ has a symmetry and, consequently, the regularity strip includes also the real v axis. Now let us take the Fourier transform to get

$$\frac{d^2\hat{u}^s}{dx_2^2} - \gamma^2(v)\hat{u}^s = 0, \quad v \in L \tag{4.5}$$

$$\gamma(v) = \sqrt{v^2 - k^2} \tag{4.6}$$

A solution to (4.5) can be obtained very easily and one writes

$$\hat{u}^s(\nu, x_2) = A(\nu)\, e^{-\gamma x_2} \quad , \quad x_2 \geq 0 \tag{4.7}$$

With the radiation condition taken into account.Here A is a coefficient to be determined. Since the function $u^s(x_1, x_2)$ is known on the line x_2=l, one can calculate its Fourier transform $\hat{u}^s(\nu, l)$ through the relation (4.3). Putting $\hat{u}^s(\nu, l)$ in (4.7) for x_2 =l allows us to obtain the coefficient A very easily.One gets

$$A = e^{\gamma l}\ \hat{u}^s(\nu, l) \tag{4.8}$$

Since the coefficient A is known, we can know write the field distribution

$$u^s(x_1, 0) = \frac{1}{2\pi} \int_L A e^{i\nu x_1} d\nu \tag{4.9}$$

And its derivative

$$\frac{\partial u^s(x_1, 0)}{\partial x_2} = \frac{1}{2\pi} \int_L -\gamma A e^{i\nu x_1} d\nu \tag{4.10}$$

On the plane x_2=0.

4.2 Description Of Iterative Method

We now seek a sequence of approximations to the unknown boundary of the obstacle. To describe the procedure which generates these approximations, let us rewrite (4.2);

$$u^s(x_1, 0) = -\frac{i}{4} \int_{\partial_{D_0}} H_0^{(m)}(k_2 \,|\, x_m - y_m \,|) \psi_y ds(y) \tag{4.11}$$

$$u^s(x) + u^0(x) = 0 \quad , x \in \partial D \tag{4.12}$$

Firstly, we make an initial guess of the unknown boundary curve ∂D of the obstacle. This guess is denoted by ∂D_0 .Let us choose a point x_0 on ∂D_0 . Then (4.11), with index m = 0, only one parameter's value we do not know, ψ_y. From (4.11) and (4.12) we can find ψ ;

$$A\psi = u_s$$

$$A^{-1}A\psi = A^{-1}u_s \;; \qquad A^{-1}A = I$$

$$\psi = A^{-1}u_s \tag{4.13}$$

After this we will find far field pattern with using ψ .

$$F(\partial D^{(m)}, \psi) = u_\infty \tag{4.14}$$

Equation (4.14) is a non-lineer equation and we can solve this equation with Newton method.

$$F(\partial D_m, \psi) + F'(\partial D_m, \psi) \cdot \Delta D = u_\infty \tag{4.15}$$

In this equation F' is far field pattern's frechet derivative. And also $\Delta D = D - D_0$.

The iterative procedure is the following:

1. Choose a closed curve ∂D_0 .

2. From equation (4.11) and (4.13) we find ψ .

3. From equation (4.15) we find ΔD .

4. We find ∂D_1 from the ψ equation.

5. We can calculate ∂D_2 from ∂D_1 and ψ . After this we find the new shape. (∂D_2)

6. The procedure then continues by iterating the steps.

5. NUMERICAL RESULTS

In this section we will give some examples aimed at electromagnetic imaging of conducting objects buried under a half space.

First we will to find the scattered field at the half-space interface by comparing exact scatered field with scatered field which calculated on the surface by analytic continuation method. Also, in this section we will see the effects of some parameters such as height (h), λ.

In the second section we present the result for imaging of conducting a object buried under a half space.

5.1 Finding the scattered field

This section is concerned to illustrate the performance of the analytic continuation method with the numerical examples. Also, we will compare this examples with the exact scattered field.

To see the effect of length of measurement line we change the value of this parameters and find the fields. In figure 5.1, we can see the exact scattered field and calculated scattered field by continuous method on the surface of an perfectly conducting cylinder. In this example we consider a situation in which f_r=300 MHz; x_2=0.2m; $\varepsilon_0 = 10^{-9}/(36*\pi)$; $k_1=\omega*\sqrt{\varepsilon_0\mu_0}$, and measurament length L= $40\lambda_0$ to see the effect of L.

In figure 5.2 , we can see the exact scattered field and calculated scattered field by continuous method on the on the same object using the same frequency, same ε_0, sane μ_0, same ω but this time we change the measurement length to the value $20\lambda_0$ to see the effect of L.

Last of all from figure 5.1 and figure 5.2 we can see that when we use L=$40\lambda_0$, we get better results.

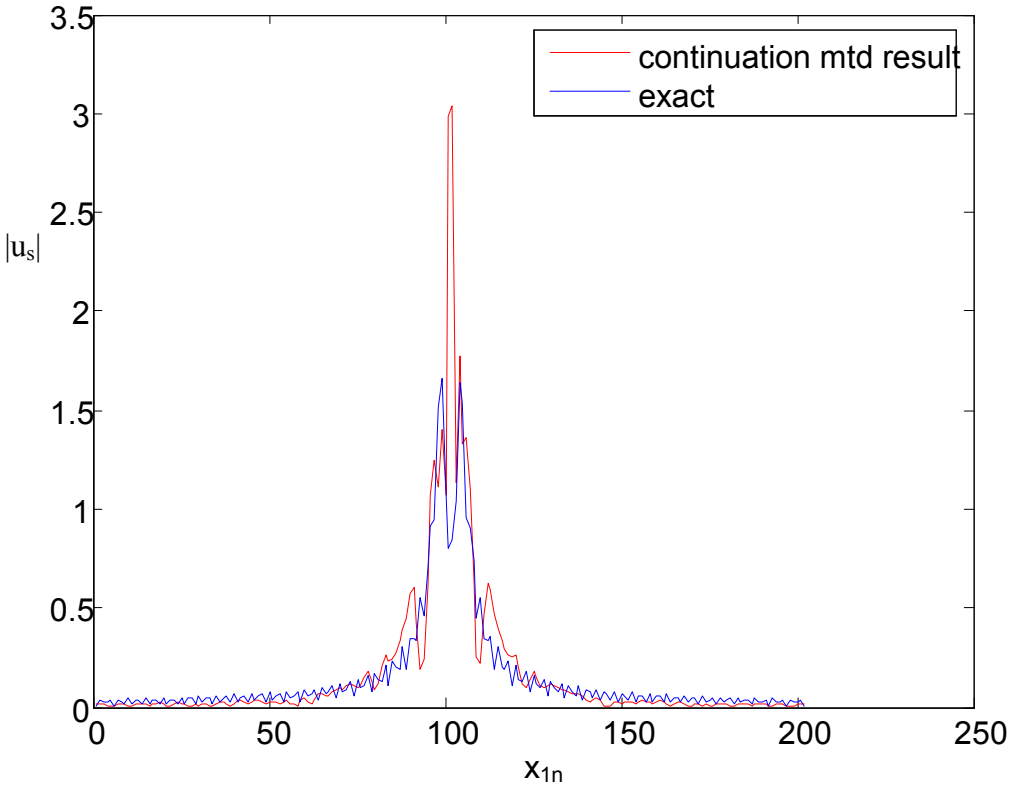

Figure 5.1: Exact total field and calculated field on the surface by analytic continuation method for measurement length L = 40 λ_0

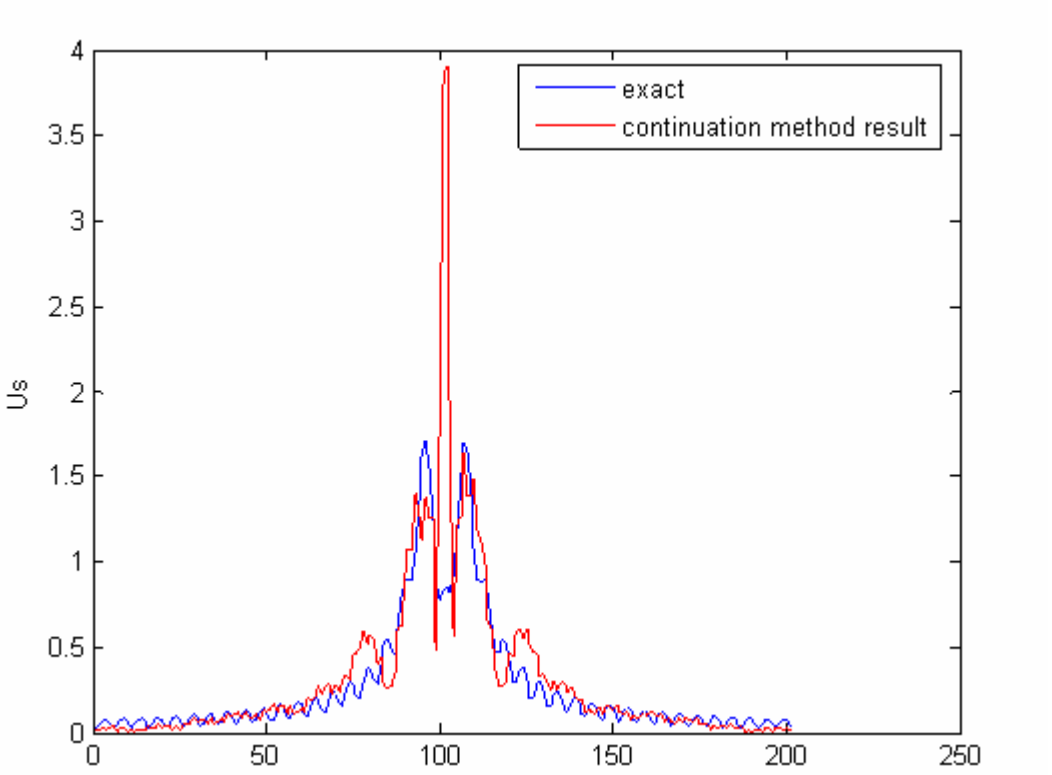

Figure 5.2: Exact total field and calculated field on the surface by analytic continuation method for measurament length L = 20 λ_0

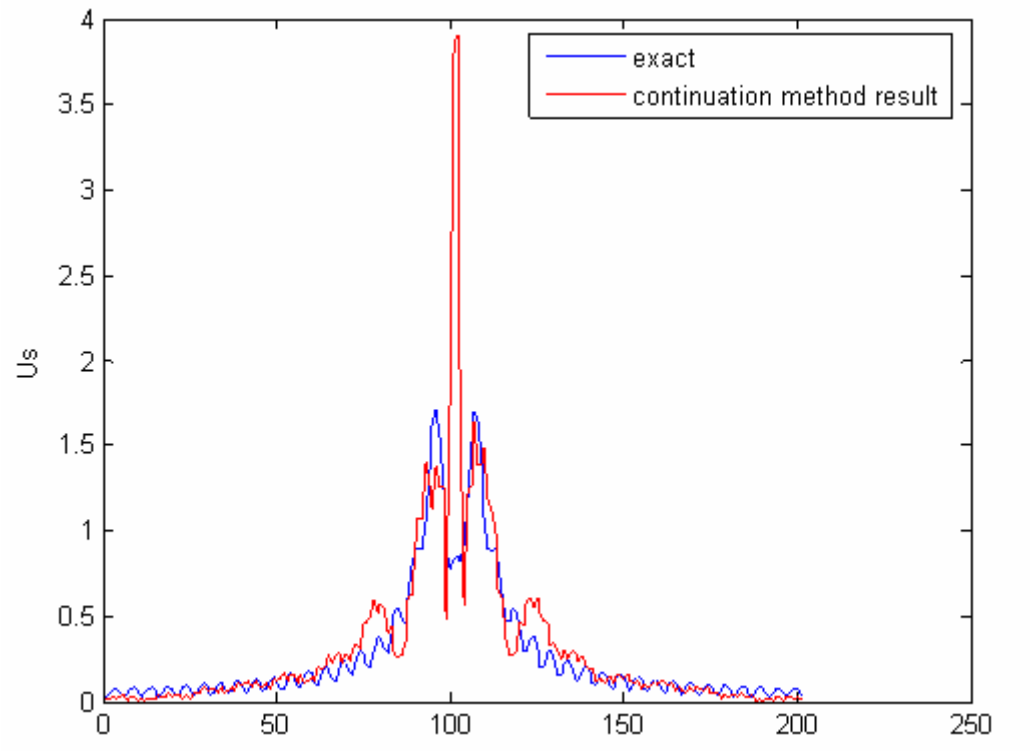

Figure 5.3 Exact total field and calculated field on the surface by analytic continuation method for $k_1 = k_0$.

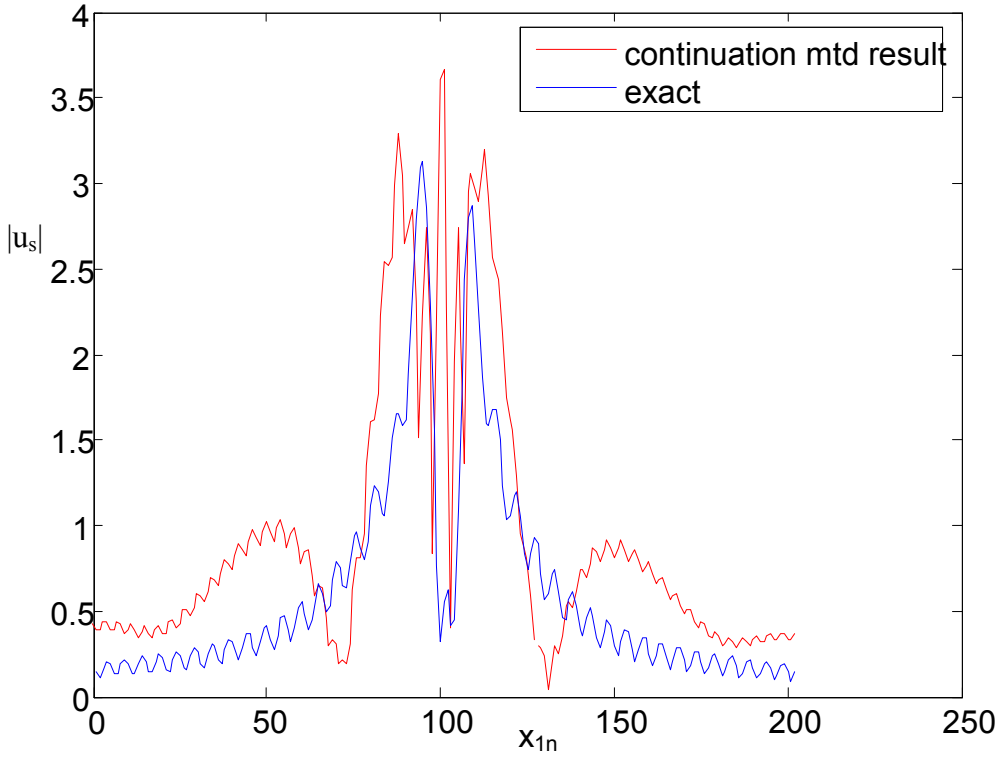

Figure 5.4 Exact total field and calculated field on the surface by analytic continuation method for $k_1 = 1.5k_0$

To see the effect of k_1 we change the value of this parameters and find the fields. In figure 5.3 , we can see the exact scattered field and calculated scattered field by continuous method on the on the same object using the same frequency, same L, same ω but this time we change k_1 to the value k_0 to see the effect of k_1.

In figure 5.4 , we can see the exact scattered field and calculated scattered field by continuous method on the on the same object using the same frequency, same L, same ω but this time we change k_1 to the value $1.5k_0$.

From figure 5.3 and figure 5.4 we can see that when we use $k_1 = k_0$, we get better results.

Finally, for this problem the best condition is fr = 300 MHz; x_2=0.2m; $k_1 = k_0$; and measurament length $L=20\lambda_0$.

5.2 Finding the shape of the buried objects

This section is concerned to illustrate the performance of the iterative method with the numerical examples. Also, we will compare this examples with the exact shape of the buried object. We find two different objects shape with this method (Ellipse, Cylinder). For each of them, first the exact scattered field data used to find the shape of the objects for iteration numbers 3-7-15, then the data which was found by continuous result method is used (Noised data). Because of this we can see the effect of iteration number to fşnd the shape of the objects.

In the first example, the buried objects shape is ellipse (x_1=0.4 ,x_2=0.3). Firstly exact scattered field is used to find the shape of the object.

In figure 5.5, we consider to find the shape of an ellipse (x_1=0.4 ,x_2=0.3) after 3 iterations. Also, to find the shape of the data we use the exact scattered field. As you see in the figure the shape is not good enough. Because of this we will increase the iteration number to find the shape of object better.

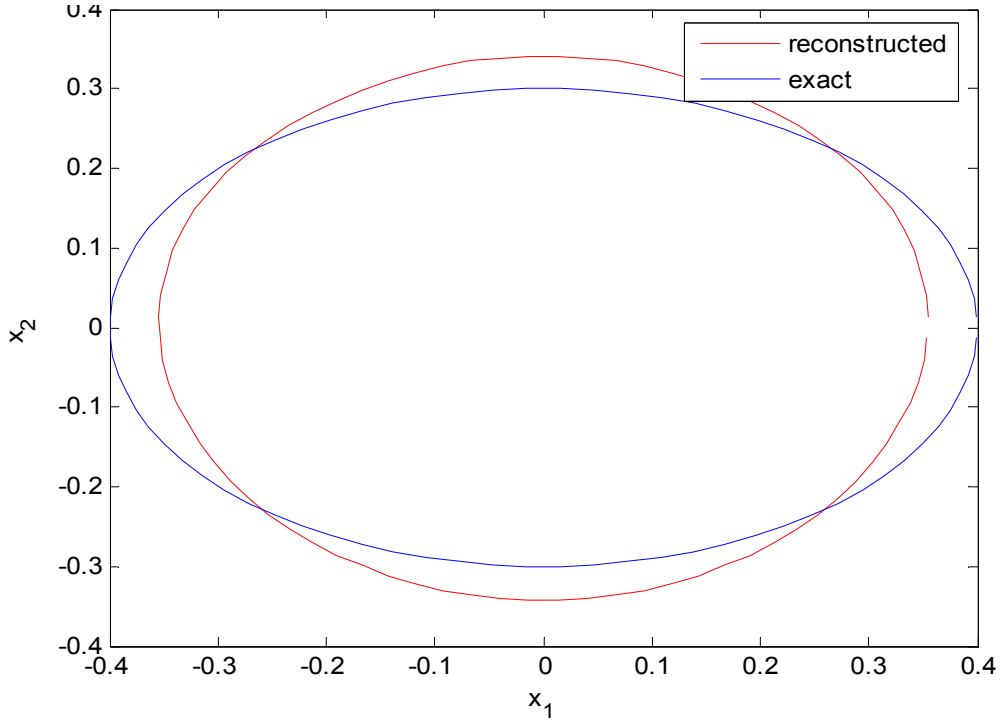

Figure 5.5: The shape of the buried object after 3 iterations using the exact scattered field

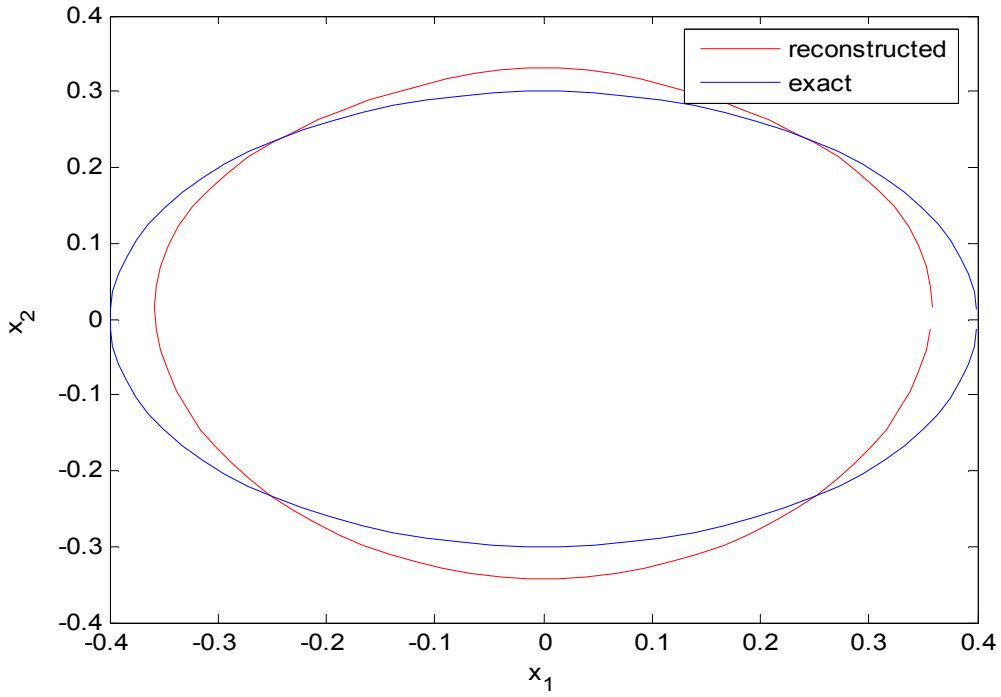

Figure 5.6: The shape of the buried object after 7 iterations using exact scattered field

In figure 5.6, we can see the same objects shape after 7 iterations. It can be seen that when we increase the iteration numbers the exact and reconstructed shapes become more closer.

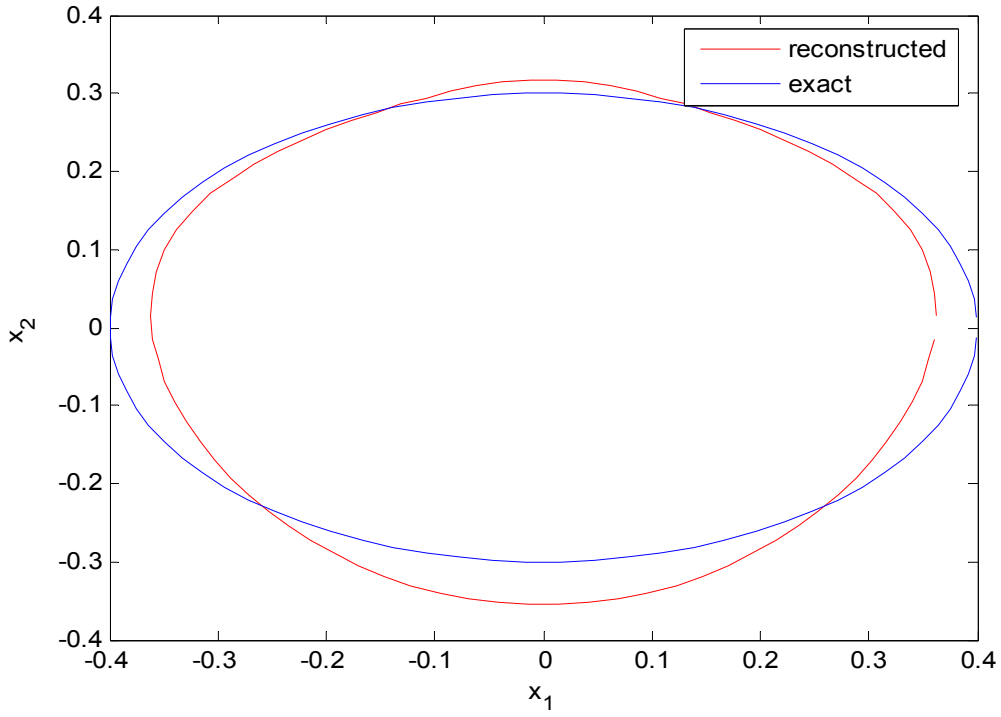

Figure 5.7: The shape of buried object after 15 iterations using the exact scattered field

In figure 5.7, we can see the same objects shape after 15 iterations. Again it can be seen that when we increase the iteration numbers the exact and reconstructed shapes become more closer. We can again increase the iteration number but after 15 iterations the objects shape that we found does not change.

After this, we will see the results when we use noise of the same form is added to the far-field patern. In figure 5.8, the result after 3 iterations is illustrated. In figure 5.9, the result after 3 iterations is illustrated. And in figure 5.10, the result after 15 iterations is illustrated. We will use the same parameters only the scattered field will change. The scattered far field which is found with analytic continuous result will be used in this examples.

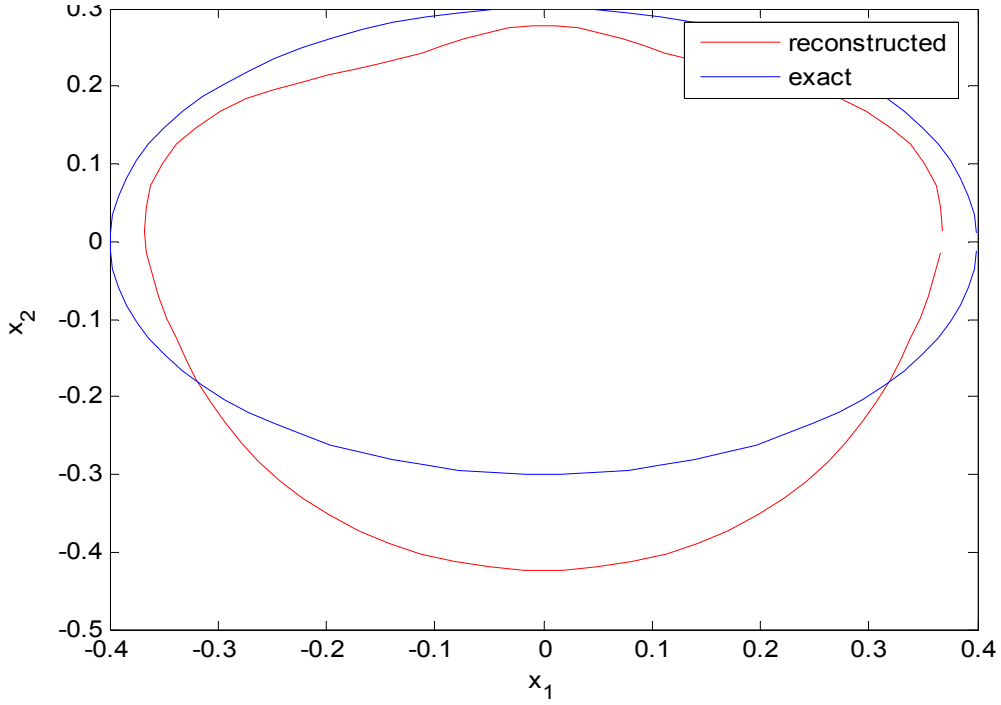

Figure 5.8: The shape of the buried object after 3 iterations using the noise added scattered field

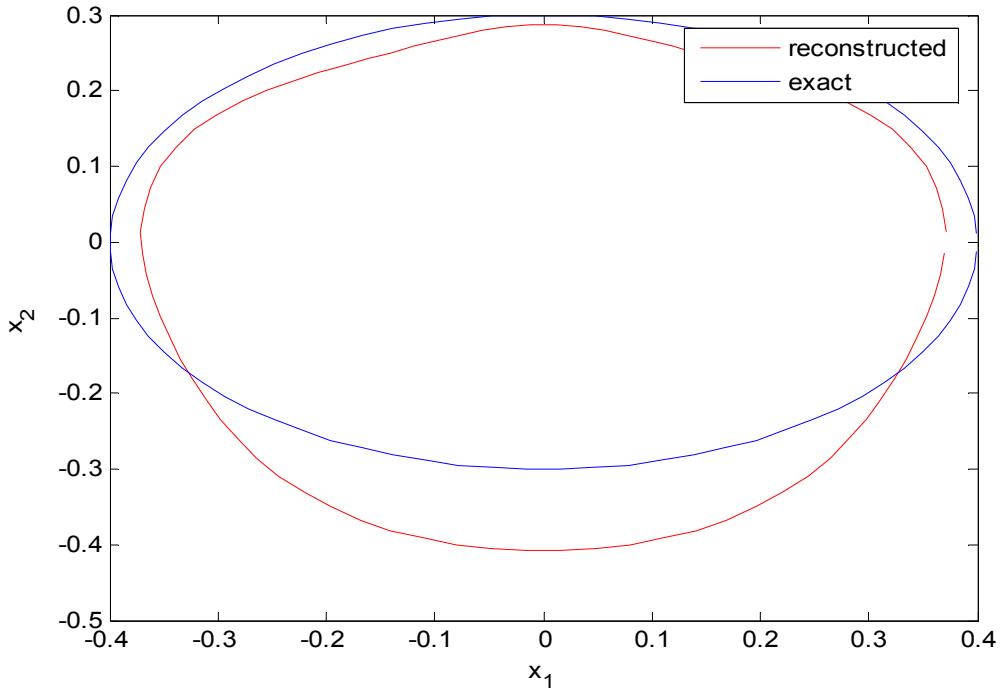

Figure 5.9: The shape of the buried object after 7 iterations using the noise added scattered field

In figure 5.8, we consider to find the shape of an ellipse (x_1=0.4 ,x_2=0.3) after 3 iterations. But this time to find the shape of the data we use the scattered field that we find from continuous method. Again the shape that we find is not good enough. We will increase the iteration number.

In figure 5.9, we can see the same objects shape after 7 iterations using the noise added scattered field. It can be seen that when we increase the iteration numbers the exact and reconstructed shapes become more closer.

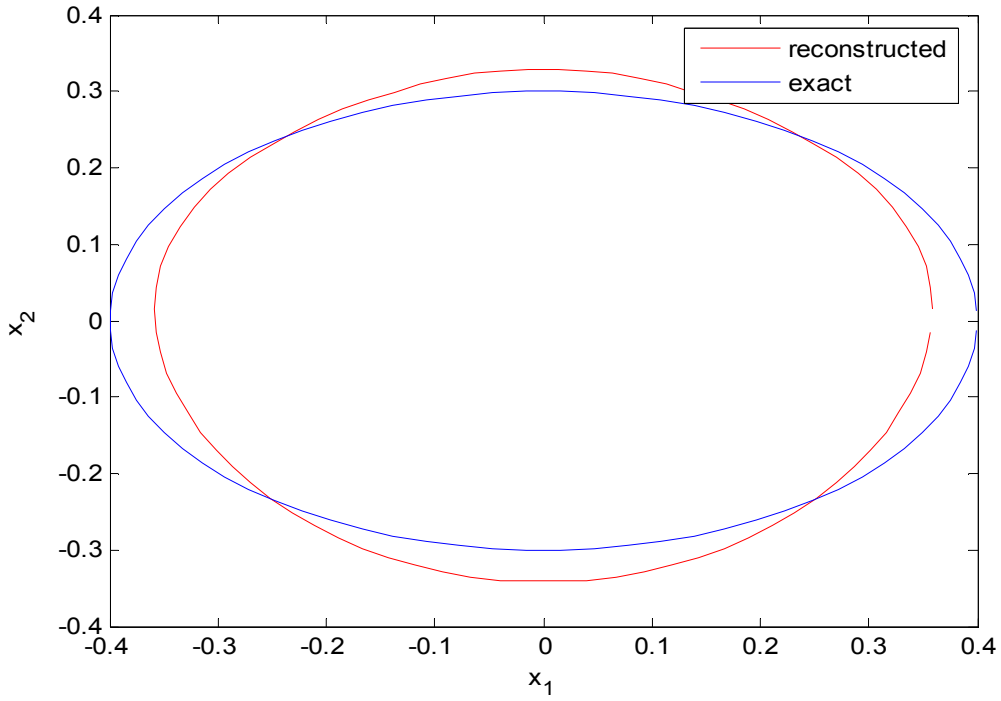

Figure 5.10: The shape of the buried object after 15 iterations using the noise added scattered field

In figure 5.10, we can see the same objects shape after 15 iterations using the noise added scattered field.Again it can be seen that when we increase the iteration numbers the exact and reconstructed shapes become more closer. But, when we use the exact data the shape is better. Because of the noise our shape is not good as the other. It can be seen that when we use the exact scattered field, our results are better.

In the second example, the buried objects shape is cylinder (r=0.4). Firstly exact scattered field is used to find the shape of the object.

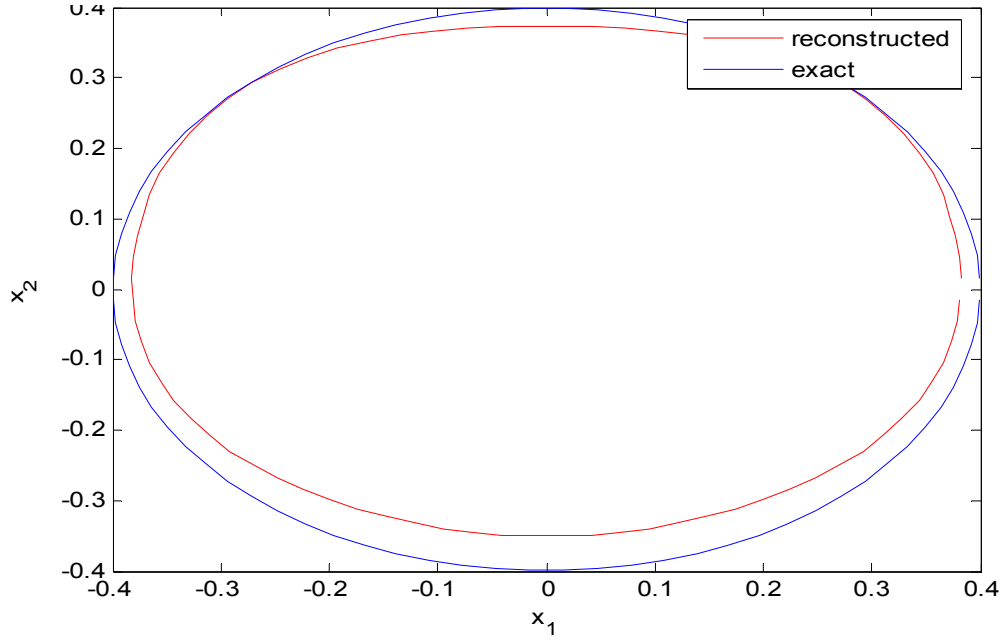

Figure 5.11: The shape of the buried object after 3 iterations using the exact scattered field

In figure 5.11, we consider to find the shape of an cylinder (r=0.4) after 3 iterations. Also, to find the shape of the data we use the exact scatered field. The shape is not good enough we will increase the iteration number.

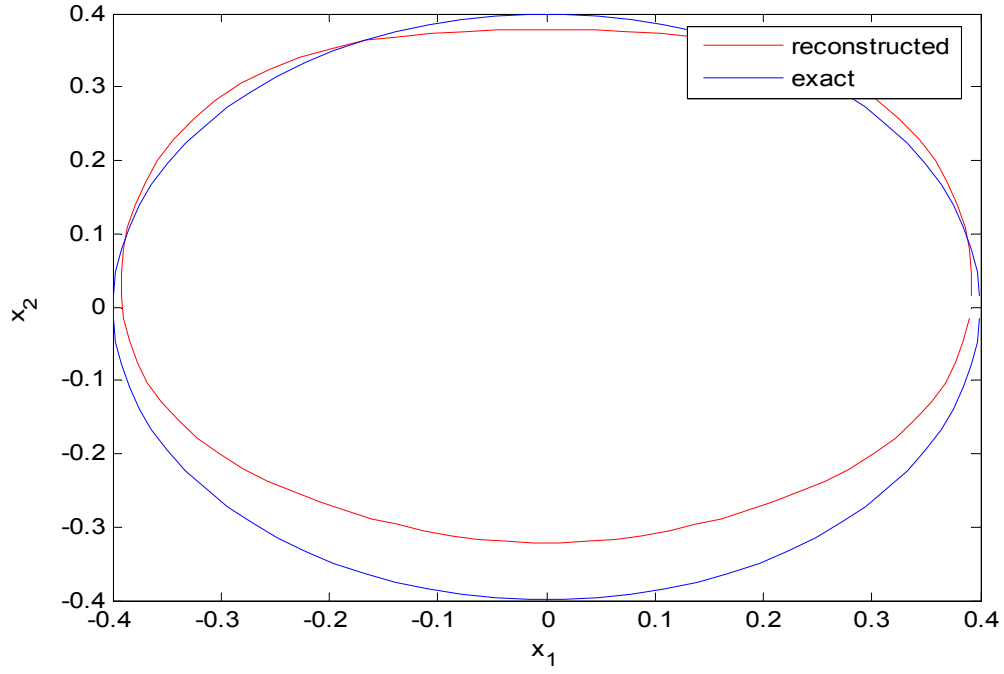

Figure 5.12: The shape of the buried object after 7 iterations using the exact scattered field

In figure 5.12, we can see the same objects shape after 7 iterations. It can be seen that when we increase the iteration numbers the exact and reconstructed shapes become more closer.

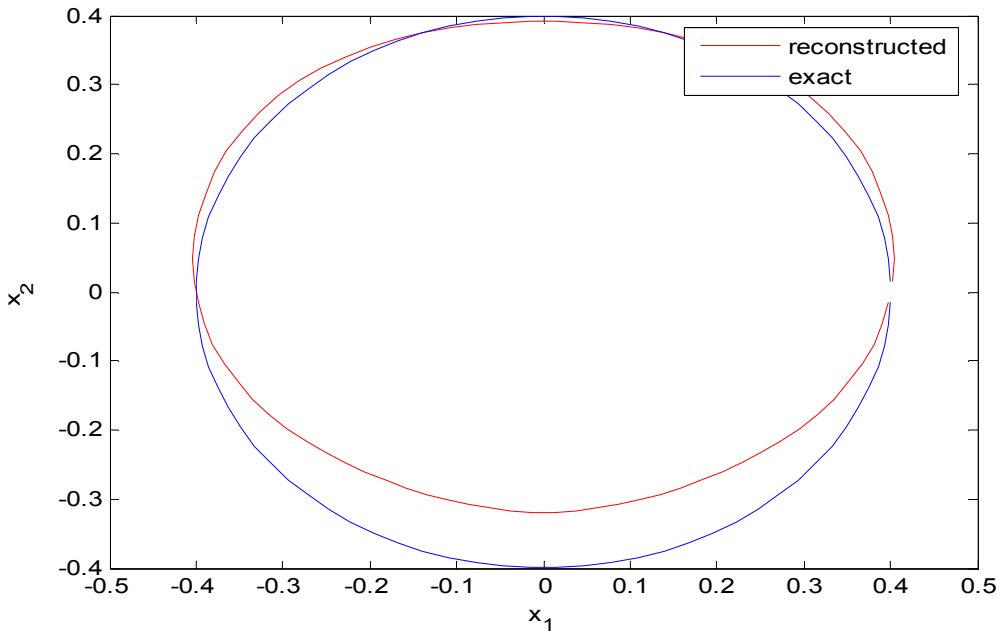

Figure 5.13: The shape of the buried object after 15 iterations using the exact scattered

In figure 5.13, we can see the same objects shape after 15 iterations.Again it can be seen that when we increase the iteration numbers the exact and reconstructed shapes become more closer.

After this, noise of the same form is added to the far-field patern , the result after 3-7-15 iterations is illustrated in Fig. 5.14, Fig 5.15, Fig 5.16.

In figure 5.14, we consider to find the shape of an cylinder (r=0.4) after 3 iterations. But this time to find the shape of the data we use the scattered field that we find from continuous method. The shape is not good enough we will increase the iteration number.

In figure 5.15, we can see the same objects shape after 7 iterations using the noise added scattered field. It can be seen that when we increase the iteration numbers the exact and reconstructed shapes become more closer.

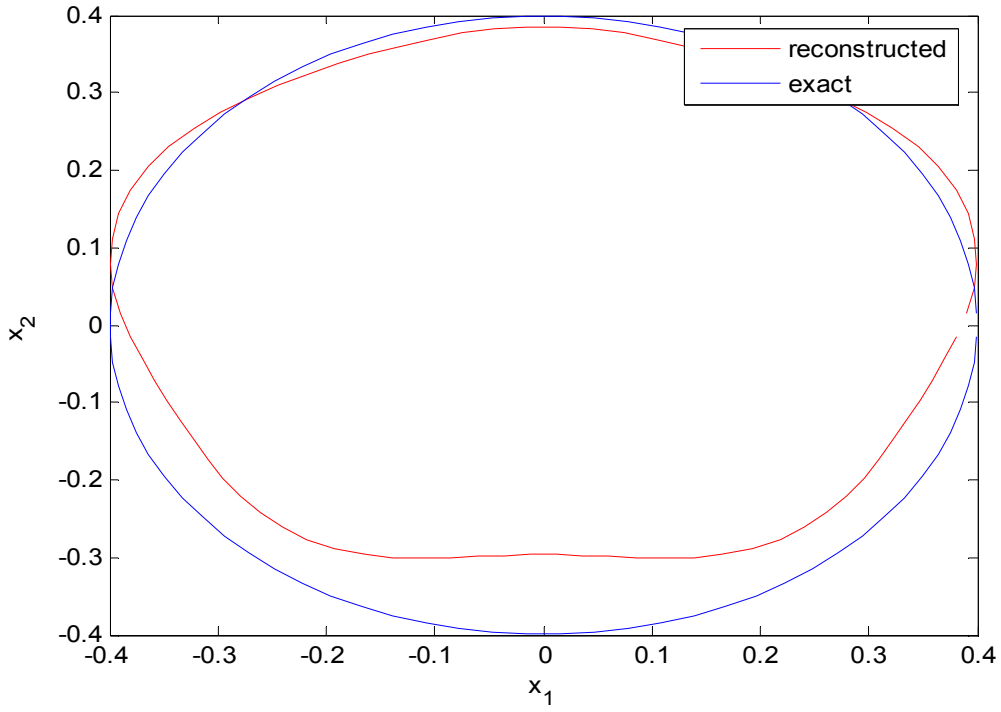

Figure 5.14: The shape of the buried object after 3 iterations using the noise added scattered field

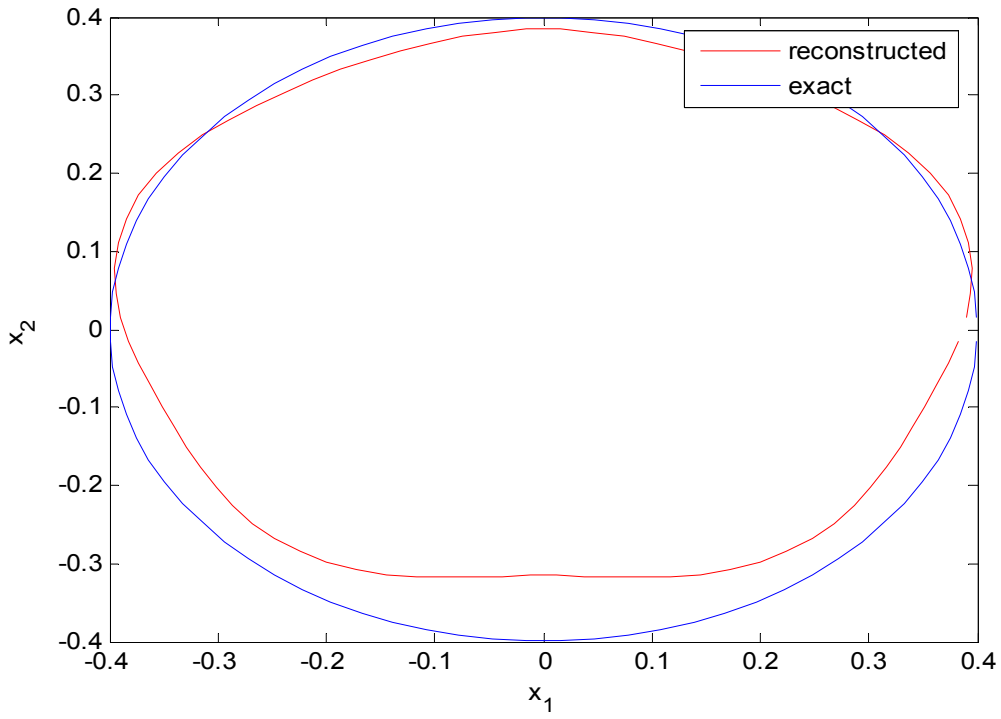

Figure 5.15: The shape of the buried object after 7 iterations using the noise added scattered field

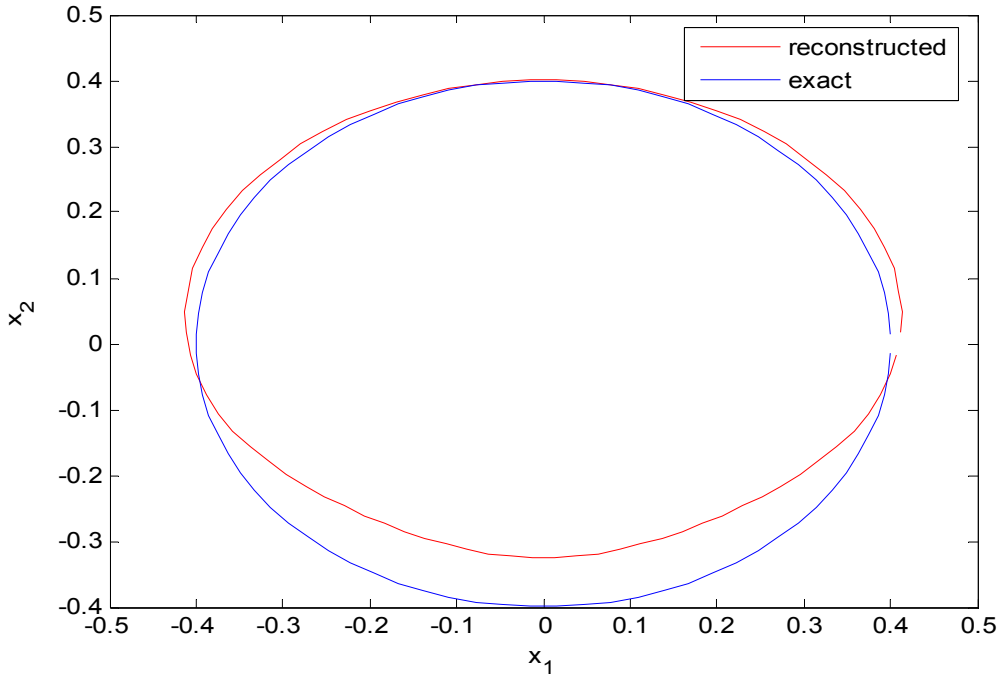

Figure 5.16: The shape of the buried object after 15 iterations using the noise added scatered field

In figure 5.16, we can see the same objects shape after 15 iterations using the noise added scattered field.Again it can be seen that when we increase the iteration numbers the exact and reconstructed shapes become more closer. But, when we use the exact data the shape is better. Because of the noise our shape is not good as the other.

6. CONCLUSION

Electromagnetic imaging of conducting objects buried under a half space by an integral equation approach has been presented. Firstly, we have find the scattered data on the upper half space. Then we find the scattered field at the half space interface. After this, we represent the the scatered field in the lower half space. At last, we have used Nyström method, Newton method and iterative method to find the shape of the buried object.

Also, it is worth to note that in the application of the method some regularization techniques have been applied since all steps the problem encountered are ill-posed.

As shown by several numerical examples, the considered approach allows to set up an efficient and reliable solution algorithm. In particular, the iterative method proves to be very stable since results obtained the same shape of the top of buried object. On the other hand the results don't give the same shape of the bottom of buried objects. All in all the numerical examples show that the approach can provide good results.

REFERENCES

[1] **Akduman, I., Kress, R., and Yapar, A**., 2006. "Iterative Reconstruction of Dielectric Rough Surface Profiles at Fixed Frequency" Inverse Problems, *No. 22, 939-954.*

[2] **Bertero, M. and Boccacci, P.,** 1998. Introduction to Inverse Problems In Imaging, Inst. Of Physics, Bristol & Philadelphia, UK.

[3] **Bucci, O. M., Crocco, L., Isernia, T. and Pascazio, V.,** 2001. Subsurface inverse scattering problems: quantifying qualifying and achieving the available information, *IEEE Trans. Geosci. Rem. Sens., 39, 2527-2538*.

[4] **Bucci, O. M., Cardace, N., Crocco, L. and Isernia, T.,** 2001. Degree of non-linearity and a new solution procedure in scalar 2-d inverse scattering problems, *J. Opt. Soc. Am. A, 18, 1832-1845.*

[5] **Bucci, O. M. and Isernia, T.,** 1997. Electromagnetic inverse scattering: retrievable information and measurement strategies, *Radio Science, 32,2123-2138.*

[6] **Colton, D. And Kress, R.** 1992. Inverse acoustic and electromagnetic scattering, Springer Verlag, Berlin.

[7] **Altuncu, Y., Yapar, A. and Akduman, I.,** 2006. On the scattering of electromagnetic waves by bodies buried in a half space with locally rough interface, *IEEE Trans. Geosci. Remote Sens. 44 1–16*

[8] **Crocco, L., Persico, R. and Soldovieri, F.**, 2002. A tomographic approach for imaging targets embedded in a layered medium, *Proc. 9th International Conference on Ground Penetrating Radar, GPR 2002,* Santa Barbara, CA, USA.

[9] **Pierri, R., Brancaccio, A., Leone, G. and Soldovieri, F.,** 2002. Electromagnetic prospection via homogeneous and inhomogeneous plane waves: the case of an embedded slab, *AEÜ, International Journal of Electronics and Communications, 56, n. 1, 11-18*.

CIRCULUM VITAE

Umut Aziz Albayrak was born in Istanbul, Turkey in 1981. He received his B.Sc degree in Electronics and Communication Engineering from Yıldız Technical University 2004. Since 2004, he is working towards M.Sc. degree in Telecommunications Engineering programme of Institude of Science and Technology at Istanbul Technical University.